PAPER • **OPEN ACCESS**

Enhancing Mechanical Properties of PETG by Optimization of Process Parameters Using the Taguchi Method

Enhancing Mechanical Properties of PETG by Optimization of Process Parameters Using the Taguchi Method

Ahmed H. Awad[1], Rehab Alaa Eldin Sayed[1] and Mohamed Atef[1]

[1] Design and Production Department, Faculty of Engineering Ain Shams University, Cairo, 11535, Egypt.
E-mail: ahmed.awad@eng.asu.edu.eg

Abstract. Fused deposition modeling is the most applied 3D printing technique in numerous fields due to its ease of use and affordability. Nowadays, polyethylene terephthalate glycol (PETG) is used as a replacement for traditional polymers due to its good chemical resistance and mechanical properties. Four process parameters were studied: nozzle temperature (210-270°C), print speed (40-200 mm/s), infill density (50-100 %), and infill pattern (Grid, Cubic, and Gyroid). However, to achieve good performance in service, it is required that the mechanical properties be maximized. Thus, this work intends to adjust the printing parameters (nozzle temperature, print speed, infill density, and infill pattern) for the PETG. Taguchi method was utilized for the experimental procedure design according to the L9 orthogonal array. After printing, the printed samples were evaluated by impact, tensile, bending, and compressive tests. Then, the ANOVA method was conducted with a 95% interval confidence level for result analysis. Optimal parameter combinations made remarkable improvements: impact strength of 28.54 KJ/m^2, yield strength of 47.27 MPa, tensile strength of 60.76 MPa, elongation of 28.96%, flexural strength of 85.42 MPa, compressive yield strength of 60.88 MPa, and a plateau stress of 56.37 MPa.

Keywords: Polyethylene Terephthalate Glycol (PETG), FDM, DOE, Taguchi, Mechanical Properties.

1. Introduction

Additive manufacturing (AM) techniques have shown a terrific potential for producing end-use products because of their material variety and the ability to manufacture complex geometries and mechanisms without needing post-processing processes or expensive tools. However, the properties of the printed parts are significantly affected by the process parameters [1].
The AM processes allow using raw materials in different forms (liquid, powder, and solid) to obtain other products for various applications. Fused deposition modeling (FDM™) is the most proper technology due to its cost-effectiveness, reliability, efficiency, high printing speed, high resolution, and easiness. Regarding the material, poly(lactic acid) (PLA) is the cheapest and most defined thermoplastic polymer available for FDM™ [2]. Also, polyethylene terephthalate (PET) is a widely produced thermoplastic polymer due to its favourable chemical stability, recyclability, processability, and ductility [3]. Moreover, polyethylene terephthalate glycol (PETG) is a glycol-modified version of PET, which is an amorphous copolyester. PETG can be transparent and resistant to crystallization, leading to the ability to be exposed to high heat levels [4].

However, the process parameters significantly impact the mechanical properties of the parts fabricated by additive manufacturing. Therefore, optimization is crucial for getting the required properties [5].
Panneerselvam et al. [6] The authors studied the flexural properties of printed PETG and the parameters of infill percentage, layer height, and infill pattern. The results revealed that increases in infill density and layer thickness increase flexural and tensile strength. The maximum strength was achieved at a hexagonal infill pattern, 0.3 mm layer height, and 80% infill percentage. Fountas et al. [7] studied the bending properties of printed PETG by varying infill density, printing temperature, speed, deposition angle, and layer height. The results revealed that the maximum flexural strength is 27.8 MPa at an infill density of 100% and the angle parallel to the x-axis. Raja et al. [8] evaluated the mechanical properties of graphene-enhanced PETG using FDM. The authors conducted an L9 orthogonal array, and the results revealed an enhancement in mechanical properties with ultimate tensile strength of 69.1 MPa, elastic modulus of 735.6 MPa, and compressive strength of 85.3 MPa. To the author's knowledge, no previous study has conducted a thermal analysis or complete mechanical characterization of PETG.
The study aims to optimize the 3D printing process for PETG material to be utilized in the casing of circuit boards using an ELEGOO Neptune 4 FDM™ 3D Printer to improve its mechanical properties. The study passed through the equipment and material preparation, choosing the key parameters, designing the experiment using Taguchi Methods, implementing tests, and optimizing the results.

2. Experimental Procedure

2.1. Material

PETG filament was selected for its strength, chemical resistance, and durability. The material was sourced from the Egyptian Mart and eSUN company. It has a diameter of 1.75 mm and a density of 1.27 gm/cm^3. Before processing, the filament underwent a drying process to remove moisture. The density of PETG filament was measured using ADAM PW 240 according to ASTM D 792. The average value of five specimens with a length of 10 mm was measured following Archimedes' principle in air and gasoline. The thermal characteristics of PETG filament were examined using thermogravimetric universal analysis (TGA) and differential scanning calorimeter (DSC). The TGA test was conducted using the TGA Q500 instrument in a nitrogen atmosphere with a flow rate of 50.0 ml/min, where a 6.5 mg sample was heated from 20℃ to 700℃ in an alumina pan with a heating rate of 10°C/min. In the DSC test, a sample of 6.5 mg was put in an aluminium pan/lid sealed by Tzero Press. The test was conducted using the DSC Q2000 calibrated by pure indium and by heating and cooling the sample from -50℃ to 300℃ three times in a nitrogen atmosphere with a heating rate of 10°C/min. The values were reported from the second heating and cooling run. The crystallization index of PETG filament was calculated by $X_c = \Delta H^* / \Delta H^o$ [9], where ΔH^* is the heat fusion of the PETG sample (J/g) estimated from the measured area of the thermogram, and ΔH^o is the heat fusion of 100% crystalline PETG. The theoretical heat of fusion 100% crystalline PET is 140 J/g [10]. To the best of the authors' knowledge, no previous research has reported the heat of fusion 100% crystalline PETG; however, PETG is a PET modified by glycol and has a low level of crystallinity [11].

2.2. Specimens Fabrication

The 3D models for the specimens were sliced using CURA 4.8 software. PETG filament was printed using an ELEGOO Neptune 4 FDM 3D Printer (China). The study considered some parameters, such as nozzle temperature (210-270°C), print speed (40-200 mm/s), infill density (50-100 %), and infill pattern (Grid, Cubic, and Gyroid), with three levels to study their effect on the mechanical properties. The selection criteria of the grid were based on the most used patterns in the industrial field. The selection criteria ensure good layer adhesion and prevent degradation and stringing. The different printing speeds affect the surface quality; high speed increases the efficiency, and low speed improves bonding. The infill density range is used to study and balance strength and weight. The grid pattern provides good strength in two directions, the cubic pattern distributes the loads evenly in three dimensions, and the gyroid pattern provides good strength-to-weight ratio and isotropic properties.

The selection of all printing parameters achieves optimal mechanical performance and environmental stability. In contrast, other parameters, such as bed temperature and layer thickness, 80℃ and 0.2 mm, respectively, were kept constant. An L_9 array of Taguchi analysis design of experiments (DOE) was implemented to avoid ambiguous conclusions, fully explore the factor interceptions, and reduce trials. Using L_9 ensures that all levels of each factor are tested, but only nine runs are required instead of 34. Table 1 shows the printing parameters and their levels, while Table 2 shows the experimental matrix of printing.

Table 1. Printing parameters and their levels.

Factor	Level 1	Level 2	Level 3
Nozzle Temperature (°C)	210	240	270
Print Speed (mm/s)	40	120	200
Infill Density (%)	50	75	100
Infill Pattern	Grid	Cubic	Gyroid

Table 2. Experimental matrix of printing.

Run	Nozzle Temp (°C)	Print Speed (mm/s)	Infill Density (%)	Infill Pattern
1	210	40	50	Grid
2	210	120	75	Cubic
3	210	200	100	Gyroid
4	240	40	75	Gyroid
5	240	120	100	Grid
6	240	200	50	Cubic
7	270	40	100	Cubic
8	270	120	50	Gyroid
9	270	200	75	Grid

2.3. Mechanical Testing

The tensile properties of printed PETG specimens were estimated according to ASTM D638 on the LR300 LLOYD machine. Average values of two specimens of Type I with a gauge length of 50 mm, width of the narrow section of 13 mm, and thickness of 3.6 mm were used. The test was executed at 25℃ with a crosshead speed of 0.5 mm/min until the fracture of the specimen.

The bending properties of the printed PETG specimens were estimated according to ASTM D790 using a three-point bending attachment on the LRX PLUS LLOYD machine. The average value of two specimens with a length of 80 mm, width of 10 mm, and thickness of 4 mm was used. The test was executed at 25℃ with a crosshead speed of 1.7 mm/min and a span length of 60 mm until failure.

The compression properties of printed PETG specimens were estimated according to ASTM D695 on the LR300 LLOYD machine. The average value of two specimens with a length of 15 mm and diameter of 10 mm was used. The test was executed at 25℃ with a 1 mm/min crosshead speed until failure.

The impact test of printed PETG specimens was conducted according to ASTM D6110 using a 2J hammer on the XJJU-5.5/50 J Izod & Charpy impact tester machine. The average value of two specimens of notched Charpy with a length of 63.5 mm, width of 12.7 mm, thickness of 4 mm, notch of 45°, and a notch depth of 2.5 mm was used.

The full dimensions of the specimens used in the mechanical tests are shown in Figure 1.

In this study, ANOVA analysis was used to identify the significant impact of the printing process of PETG.

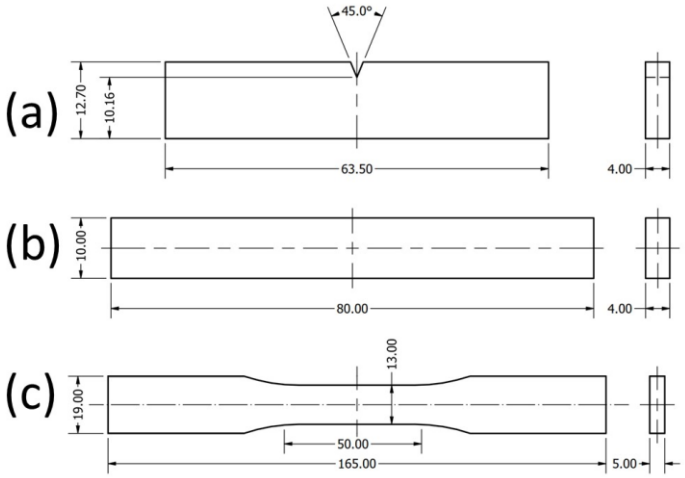

Figure 1. Dimensions of the specimens used in the mechanical tests

3. Results and Discussion

3.1. PETG Filament

The measured density of the PETG filament is 1.246 ±0.032 gm/cm^3. The thermal properties of PETG filament were characterized by TGA and DSC. The TGA curve of PETG filament, shown in Figure 2, decomposed in three steps: the range of the first step is 20.6- 353°C with a mass loss of 0.74%, the range of the second step is 353-476.4°C with a mass loss of 92.43%, while the range of the third step is 476.4-660°C with a mass loss of 6.83%.The first step may be related to the release of adsorbed water. It was reported that the second degradation step of PET corresponds to linkage decomposition. In contrast, the third step corresponds to C–C bond cleavage that leads to the formation of volatile compounds [12]. The DTG curve clearly shows the second and third peaks of the TGA curve, which demonstrates that 476.4 °C is the maximum operation temperature in 3D printing PETG filament. The DSC curve for the second cycle of PETG filament is shown in Figure 3, revealing that the onset temperature is 77.78 °C. This can be noticed by the heat fusion, represented by the peak area, which is very low, showing a crystallinity of around 1%. It was reported that PETG has relatively low levels of crystallinity [11]. Thus, the DSC thermogram showed the amorphous nature of PETG material. The thermal results of PETG filament are summarized in Table 3.

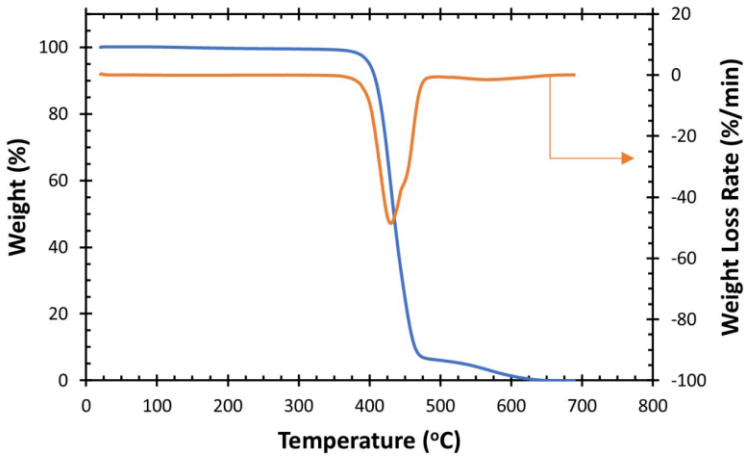

Figure 2. TGA and DTG curves of PETG filament.

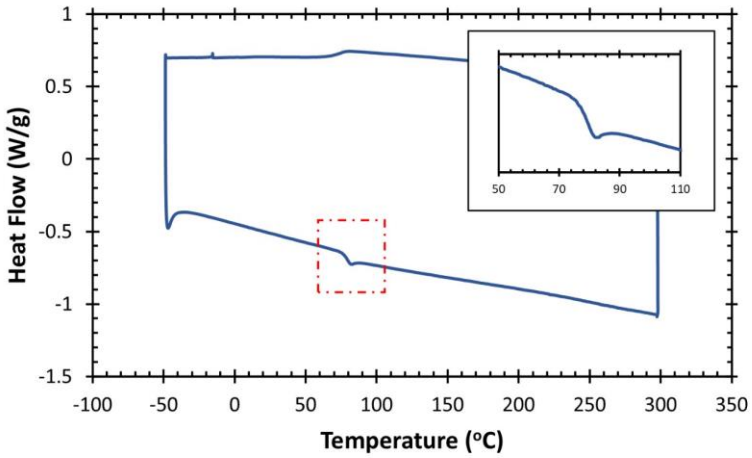

Figure 3. DSC curve of PETG filament from the second heating cycle. The peak was put as an insert.

Table 3. Thermal results of PETG filament.

Onset Temperature (°C)	**T_g (°C)**	**T_{max} (°C)**	**ΔH^* (J/g)**	**X_c (%)**
77.78	81.65	409.56	1.392	0.994

Figure 4 (a) shows the typical stress-strain curve of printed PETG specimens. The graph showed linear elastic behaviour, yielding, followed by a non-linear region reaching the maximum stress (UTS). After that, an increasing strain and a stress reduction were detected until failure occurred. Figure 4 (b) shows the typical compression stress-strain curve of printed PETG specimens. The curve showed initial linear elastic behaviour followed by a non-linear zone that ended with the yield stress. After that, the material exhibited a viscoplastic behaviour distinguished by a slight reduction in the stress (softening), reaching) a plateau with roughly constant stress, the plateau stress, followed by a significant increase in stress (strain hardening). Figure 4 (c) shows the typical stress-deflection curve for the bending test of printed PETG specimens. All specimens showed ductile phenomena in the point bending test. As the graph shows, the specimens show elastic deformation and plastic deformation reaching the maximum bending stress (flexural strength), and then stress failure occurred.

From the reported graph, it is feasible to get the maximum mechanical properties for the different studied conditions. In terms of the impact test, the maximum impact strength is 28.54 KJ/m^2 for the combination of nozzle temperature of 240℃, print speed of 120 mm/s, infill density of 100%, and infill pattern of the grid, while the maximum yield strength is 47.27 MPa for the combination of nozzle temperature of 270℃, print speed of 40 mm/s, infill density of 100%, and infill pattern of the gyroid, while the maximum tensile strength is 60.76 MPa for the same combination of yield strength of nozzle temperature of 240℃, print speed of 40 mm/s, infill density of 100%, and infill pattern of the grid, while the maximum elongation is 28.96% for the combination of nozzle temperature of 270℃, print speed of 40 mm/s, infill density of 100%, and infill pattern of the cubic. For the compression test, the behavior is similar to the tensile test, and the maximum elastic modulus is 17.64 GPa, while the maximum compressive yield strength is 60.88 MPa, and the maximum plateau stress is 56.37 MPa for a combination of nozzle temperature of 270℃, print speed of 40 mm/s, infill density of 100%, and infill pattern of the grid. In terms of the bending test, the maximum flexural strength is 85.42 MPa for the combination of nozzle temperature of 270℃, print speed of 40 mm/s, infill density of 100%, and infill pattern of the gyroid.

Table **4** shows the recommended printing parameters for each studied property.

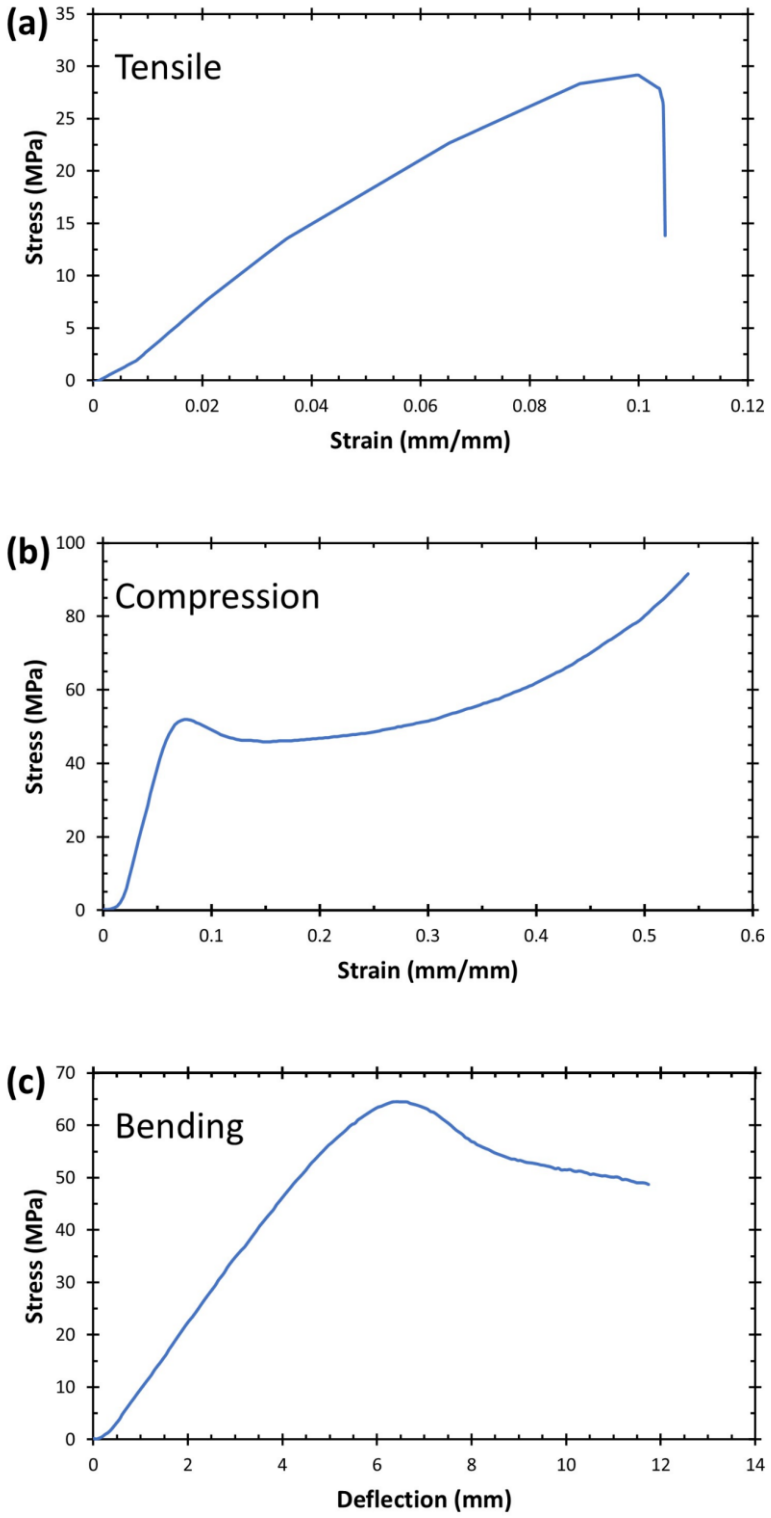

Figure 4. Typical (a) tensile stress-strain, (b) compression stress-strain, and (c) stress-deflection curves of printed PETG specimens

Table 4. Recommended conditions for a specific property

No.	Nozzle Temperature	Print Speed	Infill Density	Infill Pattern	Property
1	270	40	100	grid	compression (yield strength, elastic modulus, plateau stress)
2	270	40	100	gyroid	Tensile yield strength, flexural strength
3	270	40	100	cubic	Elongation in tensile
4	240	40	100	gyroid	Ultimate tensile strength
5	240/270	200/120	100	grid	Impact strength

Based on the ANOVA analysis, it is feasible to conclude that the infill density and infill pattern have a significant influence on the impact strength since their p-values are less than 0.05. On the other hand, all parameters (i.e., nozzle temperature, print speed, infill density, and infill pattern) significantly affect the tensile and compressive properties of PETG. Moreover, all factors significantly influence the flexural strength except the infill pattern. Figure 5 and Figure 6 show the prediction profiler based on the experimental results of the printed PETG specimens.

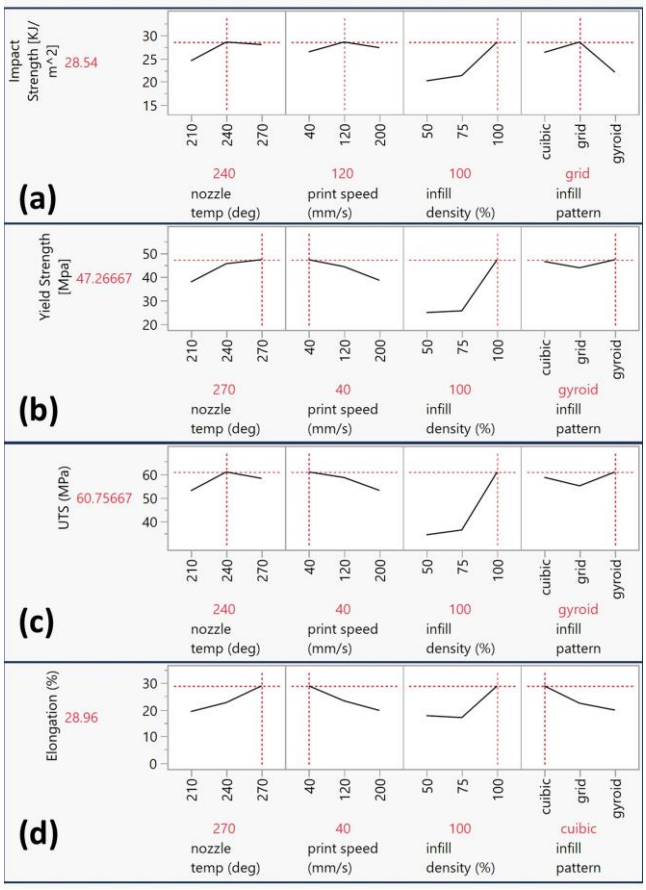

Figure 5. Prediction profiler based on the experimental results of (a) impact test and (b-d) tensile test of printed PETG specimens

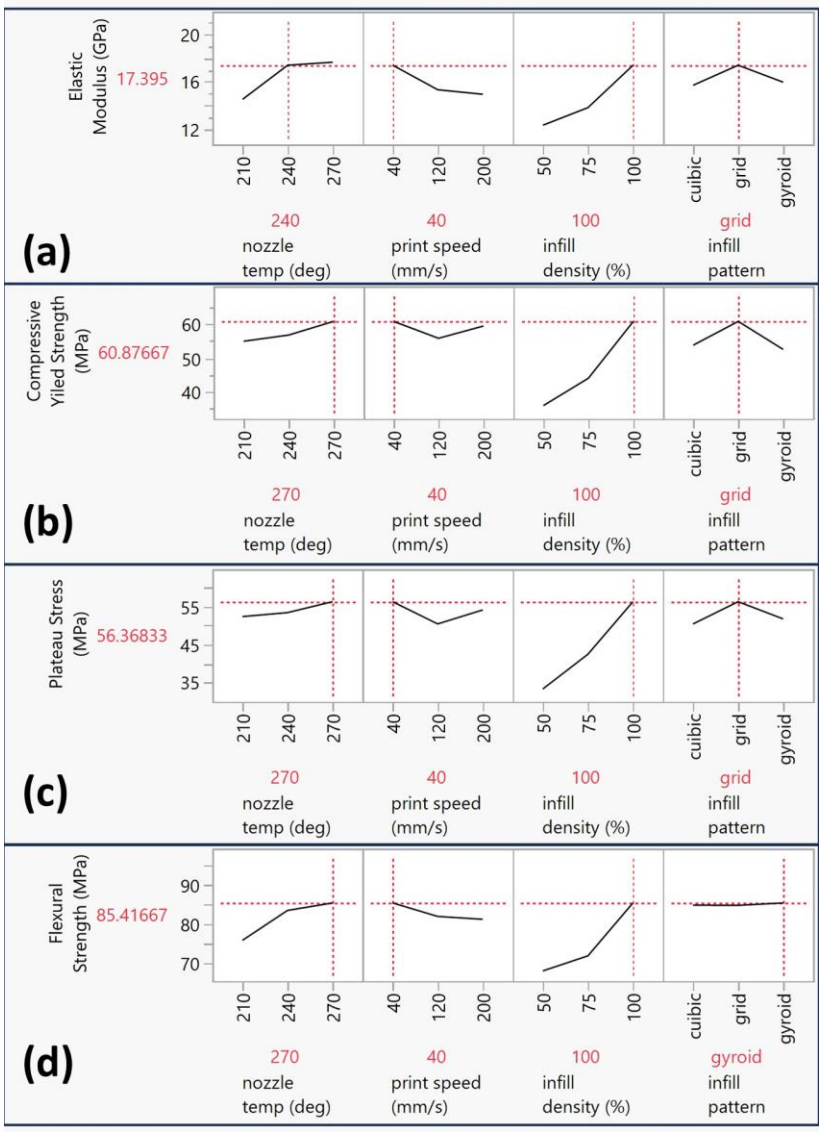

Figure 6. Prediction profiler based on the experimental results of (a-c) compression test and (d) bending test of printed PETG specimens

Figure 7 shows the effect of printing parameter interactions on the UTS of printed PETG specimens. The results revealed lower UTS was obtained at low nozzle temperatures and low printing speed due to the quick cooling and low bonding. Moreover, the UTS decreased with high nozzle temperature and speed due to weak interlayer bonds and uneven layer distribution. For example, the best combination at a print speed of 40 mm/s and a nozzle temperature of 270 °C results has the highest UTS due to the forming of strong interlayer bonds and the uniform material distribution. The infill density and patterns showed a horizontal line in the interaction, which indicates that one of the printing factors does not affect UTS at different levels of another printing factor. For example, the infill density does not affect the UTS at different print speeds, which may be related to the bonding effect overriding the high infill density effect. Moreover, the print speed does not affect the UTS at the same nozzle temperature since optimal bonding temperature may reached, making the speed variation less effective. In other words, nozzle temperature consistently affects UTS regardless of infill density and patterns. Also, the graph shows that the UTS values for different infill densities have the same trend

and do not differ. The graph shows that the UTS has the same pattern across different nozzle temperatures and printing speeds for different infill densities and patterns since the UTS is more dependent on these parameters, not infill density or pattern. This means that nozzle temperature and print speed independence affect the UTS regarding the amount of infill density or infill pattern [13].

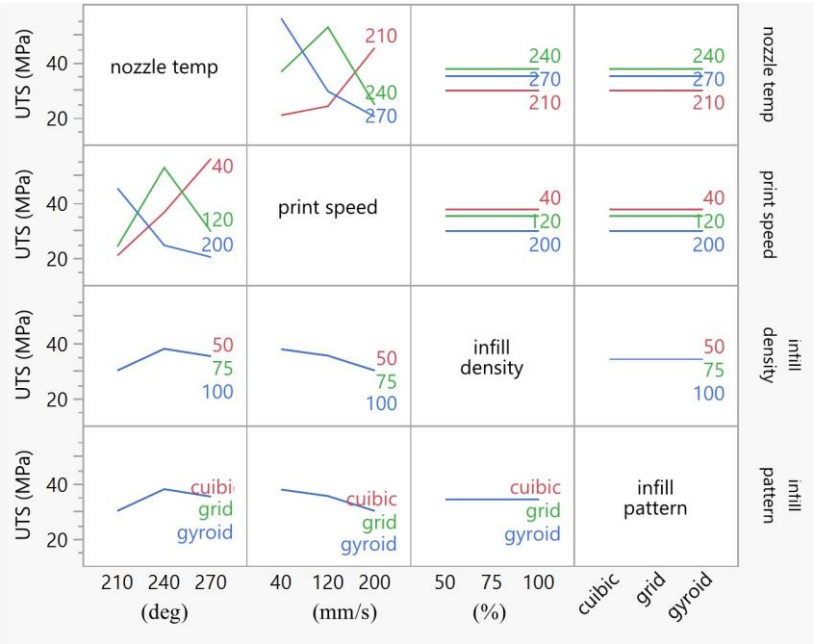

Figure 7. Interaction effects of printing parameters on UTS of printed PETG specimens

From the previous results, increasing the nozzle temperature led to enhancement of the properties, and this enhancement could be due to higher energy increases in the local temperature of the former printed layer and lower porosity, making stronger bonds between the printed layer and, accordingly, better properties [14]. Moreover, the fluidity and solidification characteristics affect the inter-bonding strength between the adjacent layers.

Regarding the printing speed, for almost all properties, increasing the printing speed leads to lower mechanical properties, which can be explained by the solidification time and the adhesion between the adjacent layers [15].

It is a fact that the mechanical properties are enhanced with increasing infill density, reaching their maximum for an infill density of 100%. It was reported that higher infill density leads to lower porosity and better interfacial bonding between the adjacent layers. On the other hand, a lower infill density has a higher porosity and weak bonding between the adjacent layers, causing weak mechanical properties. However, higher infill density leads to more dense density and higher bearing capacity, with higher consumption of the row materials [16]. Generally, PETG revealed a lower Young's Modulus value and is considered a biocompatible material. Therefore, a lower elastic modulus is needed [17].

Finally, no clear trend was obtained for all studied properties in terms of print pattern. The results show that the infill pattern significantly affects the properties in different aspects. The filling pattern affects the raster's arrangement, orientation, and bonding between the adjacent layers. The infill pattern significantly influenced the resistance against the different loads [18].

4. Conclusion

This study focused on optimizing the printing parameters of PETG material and optimizing mechanical properties to be utilized in the casing of circuit boards. The key process parameters

included nozzle temperature, print speed, infill density, and infill pattern. This study used the Taguchi method according to the L9 orthogonal array and ANOVA method for result analysis. According to the results, the following results can be concluded:

- Increasing the printing temperature greatly improves the mechanical properties of the PETG 3D-printed sample due to higher energy, lower porosity, and stronger bonds between the printed layer.
- Increasing the printing speed of PETG samples leads to lower mechanical properties due to the solidification time and the adhesion between the adjacent layers.
- Higher infill density leads to lower porosity, better interfacial bonding between the adjacent layers, and better mechanical properties, but with higher consumption of row materials.
- Infill pattern affects the mechanical properties of PETG samples due to the internal arrangement and orientation, which affect the bonding and direction of load.
- Optimal parameter combinations made remarkable improvements: impact strength of 28.54 KJ/m^2, yield strength of 47.27 MPa, tensile strength of 60.76 MPa, elongation of 28.96%, flexural strength of 85.42 MPa, compressive yield strength of 60.88 MPa, and a plateau stress of 56.37 MPa.
- Future work should focus on examining the thermal stability, electrical insulation, and flame resistance that can be utilized in the casing of circuit boards.

5. References

[1] Ngo T D, Kashani A, Imbalzano G, Nguyen K T Q and Hui D 2018 Additive manufacturing (3D printing): A review of materials, methods, applications and challenges *Compos. Part B Eng.* **143** 172–96

[2] Ronca A, Abbate V, Redaelli D F, Storm F A, Cesaro G, De Capitani C, Sorrentino A, Colombo G, Fraschini P and Ambrosio L 2022 A Comparative Study for Material Selection in 3D Printing of Scoliosis Back Brace *Materials (Basel).* **15** 5724

[3] Wang K, Shen J, Ma Z, Zhang Y, Xu N and Pang S 2021 Preparation and Properties of Poly (ethylene glycol-co-cyclohexane-1, 4-dimethanol terephthalate)/Polyglycolic Acid (PETG/PGA) Blends *Polymers (Basel).* **13** 452

[4] Yan C, Kleiner C, Tabigue A, Shah V, Sacks G, Shah D and DeStefano V 2024 PETG: applications in modern medicine *Eng. Regen.* **5** 45–55

[5] SV L S, Karthick A and Dinesh C 2024 Evaluation of mechanical properties of 3D printed PETG and Polyamide (6) polymers *Chem. Phys. Impact* **8** 100491

[6] Panneerselvam T, Raghuraman S and Vamsi Krishnan N 2021 Investigating mechanical properties of 3D-printed polyethylene terephthalate glycol material under fused deposition modeling *J. Inst. Eng. Ser. C* **102** 375–87

[7] Fountas N A, Papantoniou I, Kechagias J D, Manolakos D E and Vaxevanidis N M 2021 Experimental investigation on flexural properties of FDM-processed PET-G specimen using response surface methodology *MATEC Web of Conferences* vol 349 (EDP Sciences) p 1008

[8] Raja S, Jayalakshmi M, Rusho M A, Selvaraj V K, Subramanian J, Yishak S and Kumar T A 2024 Fused deposition modeling process parameter optimization on the development of graphene enhanced polyethylene terephthalate glycol *Sci. Rep.* **14** 30744

[9] Awad A H, El-gamasy R, A. Abd El-Wahab A and Hazem Abdellatif M 2019 Mechanical behavior of PP reinforced with marble dust *Constr. Build. Mater.* **228** 116766

[10] Cadete M S, Gomes T E P, Carvalho P J and Neto V F 2021 Polymeric foams from recycled thermoplastic poly (ethylene terephthalate) *J. Cell. Plast.* **57** 609–22

[11] Romeijn T, Behrens M, Paul G and Wei D 2022 Instantaneous and long-term mechanical properties of Polyethylene Terephthalate Glycol (PETG) additively manufactured by pellet-based material extrusion *Addit. Manuf.* **59** 103145

[12] Achagri G, Essamlali Y, Amadine O, Majdoub M, Chakir A and Zahouily M 2020 Surface modification of highly hydrophobic polyester fabric coated with octadecylamine-functionalized

graphene nanosheets *RSC Adv.* **10** 24941–50
[13] Gulo T, Mardiyana D, Sumarno D I, Putra U N and Barat J 2025 Analysis of Print Speed Variations Effect and Nozzle Temperature on the Tensile Strength of 3D Printed TPU-95A Products *J. Konversi Energi dan Manufaktur* **10** 53–60
[14] Valvez S, Silva A P and Reis P N B 2022 Optimization of printing parameters to maximize the mechanical properties of 3D-printed PETG-based parts *Polymers (Basel).* **14** 2564
[15] Berretta S, Davies R, Shyng Y T, Wang Y and Ghita O 2017 Fused Deposition Modelling of high temperature polymers: Exploring CNT PEEK composites *Polym. Test.* **63** 251–62
[16] Kumar K S, Soundararajan R, Shanthosh G, Saravanakumar P and Ratteesh M 2021 Augmenting effect of infill density and annealing on mechanical properties of PETG and CFPETG composites fabricated by FDM *Mater. Today Proc.* **45** 2186–91
[17] Shilov S Y, Rozhkova Y A, Markova L N, Tashkinov M A, Vindokurov I V and Silberschmidt V V 2022 Biocompatibility of 3D-printed PLA, PEEK and PETG: adhesion of bone marrow and peritoneal lavage cells *Polymers (Basel).* **14** 3958
[18] Akhoundi B and Behravesh A H 2019 Effect of filling pattern on the tensile and flexural mechanical properties of FDM 3D printed products *Exp. Mech.* **59** 883–97